ISPACS 2006

2006 International Symposium on Intelligent Signal Processing and Communication Systems (ISPACS2006)
Yonago Convention Center, Tottori, Japan

A Phase-Based Palmprint Recognition Algorithm and Its Experimental Evaluation

Koichi Ito, Takafumi Aoki
Graduate School of Information Sciences,
Tohoku University,
Sendai 980–8579, Japan
E-mail: ito@aoki.ecei.tohoku.ac.jp

Hiroshi Nakajima, Koji Kobayashi
Yamatake Corporation,
Isehara 259–1195, Japan

Tatsuo Higuchi
Faculty of Engineering,
Tohoku Institute of Technology,
Sendai 982–8577, Japan

***Abstract*— A palm, a large inner surface of a hand, contains pattern of ridges and valleys much like a fingerprint. The palmprint is expected to be more distinctive than the fingerprint, since the area of the palm is much larger than that of the finger and the palm has additional distinctive features such as principle lines, ridges, minutiae points, singular points and texture. This paper presents a palmprint recognition algorithm using phase-based image matching. The use of the phase components in 2D (two-dimensional) discrete Fourier transforms of palmprint images makes possible to achieve highly robust palmprint recognition. Experimental evaluation using palmprint images clearly demonstrates an efficient matching performance of the proposed algorithm.**

I. Introduction

Biometric authentication has been receiving much attention over the past decade with increasing demands in automated personal identification. Among many biometric techniques, palmprint recognition is one of the most reliable approaches, since a palmprint, the large inner surface of a hand, contains many features such as principle lines, ridges, minutiae points, singular points and texture [1]. The limited works on plamprint recognition are reported since palmprint recognition is a relatively new biometric authentication technique.

Previous works are based on feature-based matching which is to extract feature vectors corresponding to individual palmprint images and perform palmprint matching based on some distance metrics [1], [2]. One of the difficult problems in feature-based palmprint recognition is that the matching performance is significantly influenced by many parameters in feature extraction process, which may vary depending on environmental factors of palmprint image acquisition.

This paper presents an efficient algorithm for palmprint recognition using phase-based image matching — an image matching technique using the phase components in 2D Discrete Fourier Transforms (DFTs) of given images. The technique has been successfully applied to sub-pixel image registration tasks for computer vision applications [3], [4], [5]. In our previous work [6], [7], [8], we have proposed a fingerprint recognition algorithm using phase-based image matching, which has already been implemented in actual fingerprint verification units [9]. We also have proposed an iris recognition algorithm using phase-based image matching [10], [11].

In this paper, we present that the same technique is also highly effective for palmprint recognition. The use of phase information makes possible to achieve highly robust palmprint recognition. Experimental evaluation using palmprint databases clearly demonstrates an efficient matching performance of the proposed algorithm.

II. Phase-Based Image Matching

In this section, we introduce the principle of phase-based image matching using the Phase-Only Correlation (POC) function (which is sometimes called the "phase-correlation function") [3], [4], [5]. Consider two $N_1 \times N_2$ images, $f(n_1, n_2)$ and $g(n_1, n_2)$, where we assume that the index ranges are $n_1 = -M_1, \cdots, M_1$ ($M_1 > 0$) and $n_2 = -M_2, \cdots, M_2$ ($M_2 > 0$) for mathematical simplicity, and hence $N_1 = 2M_1 + 1$ and $N_2 = 2M_2 + 1$. Let $F(k_1, k_2)$ and $G(k_1, k_2)$ denote the 2D DFTs of the two images. $F(k_1, k_2)$ is given by

$$\begin{aligned} F(k_1, k_2) &= \sum_{n_1, n_2} f(n_1, n_2) W_{N_1}^{k_1 n_1} W_{N_2}^{k_2 n_2} \\ &= A_F(k_1, k_2) e^{j\theta_F(k_1, k_2)}, \end{aligned} \quad (1)$$

where $k_1 = -M_1, \cdots, M_1$, $k_2 = -M_2, \cdots, M_2$, $W_{N_1} = e^{-j\frac{2\pi}{N_1}}$, $W_{N_2} = e^{-j\frac{2\pi}{N_2}}$, and $\sum_{n_1, n_2}$ denotes $\sum_{n_1=-M_1}^{M_1} \sum_{n_2=-M_2}^{M_2}$. $A_F(k_1, k_2)$ is amplitude and $\theta_F(k_1, k_2)$ is phase. $G(k_1, k_2)$ is defined in the same way. The cross-phase spectrum $R_{FG}(k_1, k_2)$ is given by

$$\begin{aligned} R_{FG}(k_1, k_2) &= \frac{F(k_1, k_2)\overline{G(k_1, k_2)}}{|F(k_1, k_2)\overline{G(k_1, k_2)}|} \\ &= e^{j\theta(k_1, k_2)}, \end{aligned} \quad (2)$$

where $\overline{G(k_1, k_2)}$ is the complex conjugate of $G(k_1, k_2)$ and $\theta(k_1, k_2)$ denotes the phase difference $\theta_F(k_1, k_2) - \theta_G(k_1, k_2)$. The POC function $r_{fg}(n_1, n_2)$ is the 2D Inverse DFT (2D IDFT) of $R_{FG}(k_1, k_2)$ and is given by

$$r_{fg}(n_1, n_2) = \frac{1}{N_1 N_2} \sum_{k_1, k_2} R_{FG}(k_1, k_2) W_{N_1}^{-k_1 n_1} W_{N_2}^{-k_2 n_2}, \quad (3)$$

where $\sum_{k_1, k_2}$ denotes $\sum_{k_1=-M_1}^{M_1} \sum_{k_2=-M_2}^{M_2}$. When two images are similar, their POC function gives a distinct sharp peak. When two images are not similar, the peak drops significantly.

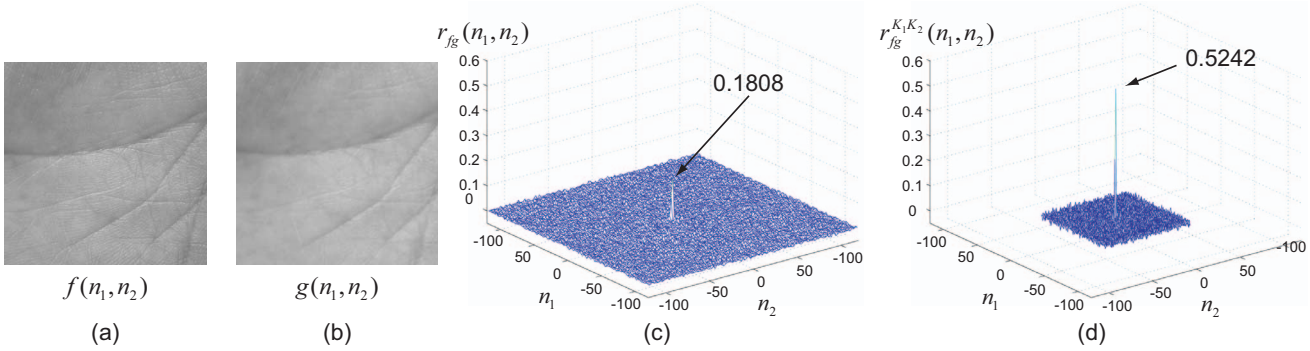

Fig. 1. Example of genuine matching using the original POC function and the BLPOC function: (a) registered palmprint image $f(n_1, n_2)$, (b) input palmprint image $g(n_1, n_2)$, (c) original POC function $r_{fg}(n_1, n_2)$ and (d) BLPOC function $r_{fg}^{K_1K_2}(n_1, n_2)$ with $K_1/M_1 = 0.40$ and $K_2/M_2 = 0.40$.

The height of the peak gives a good similarity measure for image matching, and the location of the peak shows the translational displacement between the images.

We modify the definition of POC function to have a BLPOC (Band-Limited Phase-Only Correlation) function [6] dedicated to palmprint matching tasks. The idea to improve the matching performance is to eliminate meaningless high frequency components in the calculation of cross-phase spectrum $R_{FG}(k_1, k_2)$ depending on the inherent frequency components of palmprint images. Assume that the ranges of the inherent frequency band are given by $k_1 = -K_1, \cdots, K_1$ and $k_2 = -K_2, \cdots, K_2$, where $0 \leq K_1 \leq M_1$ and $0 \leq K_2 \leq M_2$. Thus, the effective size of frequency spectrum is given by $L_1 = 2K_1 + 1$ and $L_2 = 2K_2 + 1$. The BLPOC function is given by

$$r_{fg}^{K_1K_2}(n_1, n_2) = \frac{1}{L_1 L_2} \sum_{k_1,k_2}{}' R_{FG}(k_1, k_2) W_{L_1}^{-k_1 n_1} W_{L_2}^{-k_2 n_2}, \tag{4}$$

where $n_1 = -K_1, \cdots, K_1$, $n_2 = -K_2, \cdots, K_2$, and $\sum'_{k_1,k_2}$ denotes $\sum_{k_1=-K_1}^{K_1} \sum_{k_2=-K_2}^{K_2}$. Note that the maximum value of the correlation peak of the BLPOC function is always normalized to 1 and does not depend on L_1 and L_2.

Figure 1 shows an example of genuine matching using the original POC function r_{fg} and the BLPOC function $r_{fg}^{K_1K_2}$. The BLPOC function provides the higher correlation peak and better discrimination capability than that of the original POC function.

III. Palmprint Recognition Algorithm

In this section, we present a palmprint recognition algorithm using the POC function. In previous works, the shape of a hand is used to align different palmprint images for matching [1], [2]. So, the placement of a hand has to be controlled by pegs in order to extract the central part of a palm. On the other hand, the proposed algorithm employs the high-accuracy image registration technique using phase-based image matching which can estimate scaling factor, rotation angle and translational displacement between images [4]. Hence, we can develop a palmprint recognition system without controlling the placement of a hand.

The proposed algorithm consists of the three steps: (i) scale, rotation and displacement alignment, (ii) common region extraction and (iii) palmprint matching.

A. Rotation and displacement alignment

We need to normalize scale, rotation and displacement between the registered image $f(n_1, n_2)$ and the input image $g(n_1, n_2)$ in order to perform the high-performance palmprint matching.

At first, we reduce the effect of background components in palmprint images by applying 2D spatial window to the two image $f(n_1, n_2)$ and $g(n_1, n_2)$. The 2D Hanning window is applied at the center of gravity of each palmprint to align the two images $f(n_1, n_2)$ and $g(n_1, n_2)$ correctly. The center of gravity of each palmprint is detected by using n_1-axis projection and n_2-axis projection of pixel values. Figure 2 (a) shows the palmprint images and their centers of gravity, and (b) shows the palmprint images, $f_w(n_1, n_2)$ and $g_w(n_1, n_2)$, after applying 2D Hanning window.

Next, we estimate the scaling factor λ and the rotation angle θ using the amplitude spectra of $f_w(n_1, n_2)$ and $g_w(n_1, n_2)$ as follows (see [4] for detailed discussions).

1) Calculate 2D DFTs of $f_w(n_1, n_2)$ and $g_w(n_1, n_2)$ to obtain $F_w(k_1, k_2)$ and $G_w(k_1, k_2)$.
2) Calculate amplitude spectra $|F_w(k_1, k_2)|$ and $|G_w(k_1, k_2)|$.
3) Calculate the log-polar mapping $|F_{LP}(l_1, l_2)|$ and $|G_{LP}(l_1, l_2)|$.
4) Estimate the image displacement between $|F_{LP}(l_1, l_2)|$ and $|G_{LP}(l_1, l_2)|$ using the peak location of the BLPOC function $r_{|F_{LP}||G_{LP}|}^{K_1K_2}(n_1, n_2)$ to obtain λ and θ, where $K_1/M_1 = K_2/M_2 = 0.50$.

Using λ and θ, we obtain a scale- and rotation-normalized image $g_{w\lambda\theta}(n_1, n_2)$. Then, we align the translational displacement between $f_w(n_1, n_2)$ and $g_{w\lambda\theta}(n_1, n_2)$ using the peak location of the BLPOC function $r_{f_w g_{w\lambda\theta}}^{K_1K_2}(n_1, n_2)$, where $K_1/M_1 = K_2/M_2 = 0.50$. Thus, we have normalized versions of the registered image and the input image as shown in Fig. 2 (c), which are denoted by $f'(n_1, n_2)$ and $g'(n_1, n_2)$.

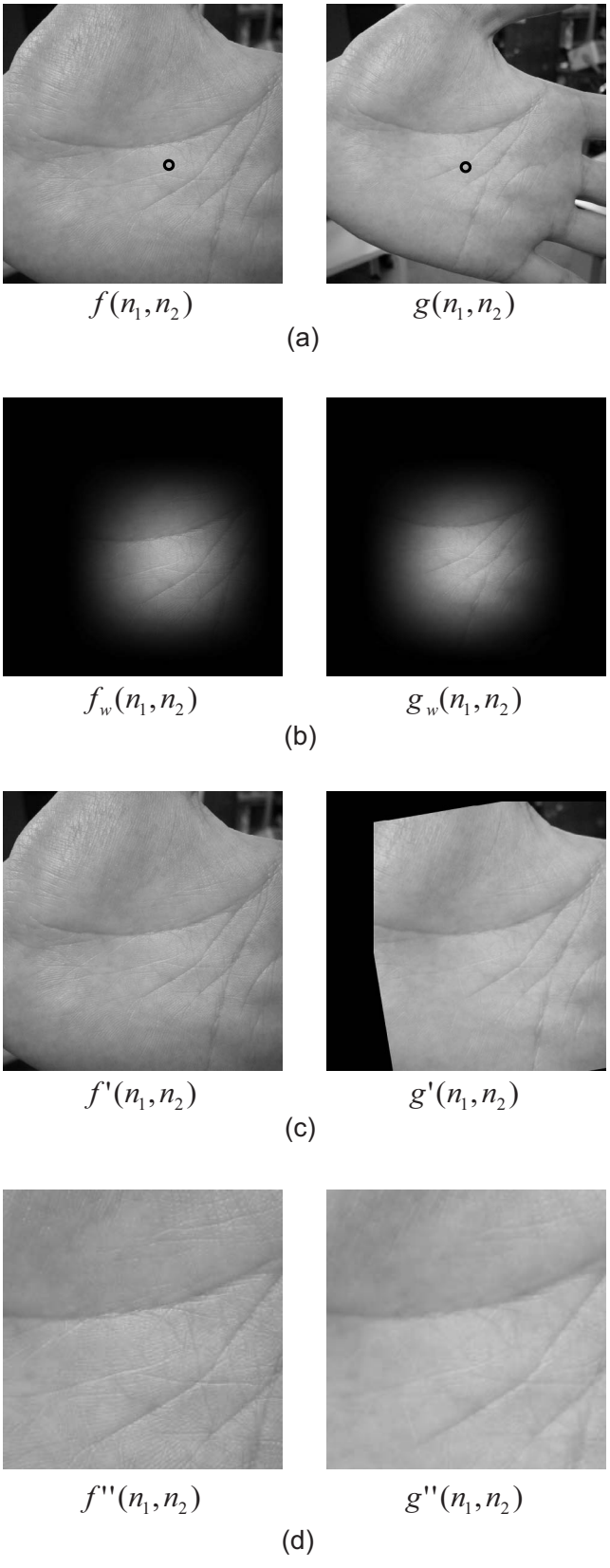

Fig. 2. Rotation and displacement alignment and common region extraction: (a) the registered image $f(n_1, n_2)$, the input image $g(n_1, n_2)$, (b) images, $f_w(n_1, n_2)$ and $g_w(n_1, n_2)$, after applying 2D Hanning window, (c) normalized images $f'(n_1, n_2)$ and $g'(n_1, n_2)$, and (d) extracted common regions $f''(n_1, n_2)$ and $g''(n_1, n_2)$.

B. Common region extraction

Next step is to extract the overlapped region (intersection) of the two images $f'(n_1, n_2)$ and $g'(n_1, n_2)$. This process improves the accuracy of palmprint matching, since the non-overlapped areas of the two images become the uncorrelated noise components in the BLPOC function. In order to detect the effective palmprint areas in the registered image $f'(n_1, n_2)$ and the input image $g'(n_1, n_2)$, we examine the n_1-axis projection and the n_2-axis projection of pixel values. Only the common effective image areas, $f''(n_1, n_2)$ and $g''(n_1, n_2)$, with the same size are extracted for the succeeding image matching step (Fig. 2 (d)).

C. Palmprint matching

We calculate the BLPOC function $r^{K_1 K_2}_{f''g''}(n_1, n_2)$ between the two extracted images $f''(n_1, n_2)$ and $g''(n_1, n_2)$, and evaluate the matching score. The matching score is the highest peak value of the BLPOC function $r^{K_1 K_2}_{f''g''}(n_1, n_2)$.

IV. Experimental Results

This section describes a set of experiments using the PolyU palmprint database (DB_A) [12] and our palmprint database (DB_B) for evaluating palmprint matching performance of the proposed algorithm.

DB_A consists of 600 images (384×284 pixels) with 100 subjects and 6 different images of each palmprint. The palmprint images in this database are taken by using the palmprint recognition system, where the placement of a hand is controlled by pegs. DB_B consists of 200 images (640×480 pixels) with 20 subjects and 10 different images of each palmprint. The images in this database are taken by using a commercially available digital camera, where the constrained condition is only that a hand is turned to the camera. Figure 3 shows some examples of palmprint images in these databases. In our experiments, the parameters of BLPOC function in the matching step are $K_1/M_1 = K_2/M_2 = 0.75$ for DB_A and $K_1/M_1 = K_2/M_2 = 0.40$ for DB_B, respectively.

The performance of the biometrics-based authentication system is evaluated by the Receiver Operating Characteristic (ROC) curve, which illustrated the Genuine Acceptance Rate (GAR) against the False Acceptance Rate (FAR) at different thresholds on the matching score. We first evaluate the GAR for all the possible combinations of genuine attempts; the number of attempts is ${}_6C_2 \times 100 = 1,500$ for DB_A and ${}_{10}C_2 \times 20 = 900$ for DB_B, respectively. Next, we evaluate the FAR impostor attempts. As for DB_A, the number of attempts is ${}_{100}C_2 = 4950$, where we select a single image (the first image) for each palmprint and make all the possible combinations of impostor attempts. As for DB_B, the number of impostor attempts is ${}_{20}C_2 \times 10^2 = 19,000$, where we select all the possible combinations of impostor attempts The performance is also evaluated by the Equal Error Rate (EER), which is defined as the error rate where $100 - \mathrm{GAR} = \mathrm{FAR}$.

We compare two algorithms: (A) a feature-based algorithm [2] and (B) the proposed algorithm. Figures 4 (a) and (b) show the ROC curves and EERs for DB_A and DB_B, respectively.

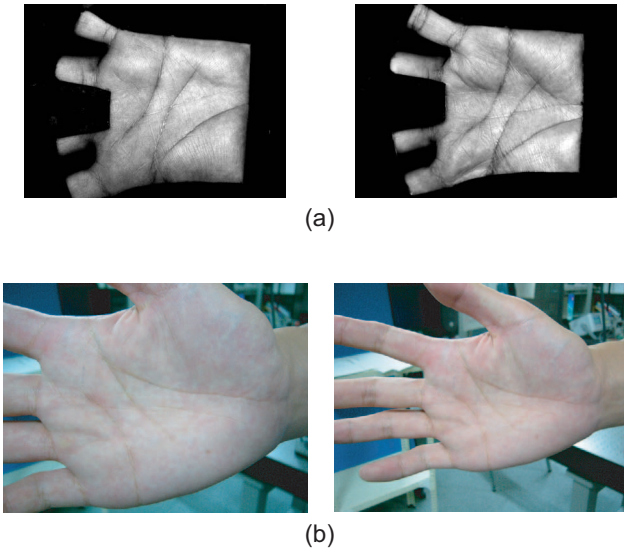

Fig. 3. Examples of palmprint images in databases: a pair of palmprint images in DB_A (a) and DB_B (b).

In both cases, the proposed algorithm (B) exhibits significantly higher performance, since its ROC curve is located at higher GAR and lower FAR region than those of the feature-based algorithm (A). As for DB_A, EER of the proposed algorithm (B) is 0.12%, while EER of the feature-based algorithm (A) is 0.45%. As for DB_B, EER of the proposed algorithm (B) is 0.57%, while EER of the feature-based algorithm (A) is 3.87%. As is observed in the above experiments, the proposed algorithm is particularly useful for verifying low-quality palmprint images.

V. Conclusion

This paper proposed a palmprint recognition algorithm using the phase-based image matching. Experimental performance evaluation demonstrates an efficient performance of our proposed algorithm compared with the feature-based algorithm. We have already demonstrated that the phase-based image matching is also effective for fingerprint and iris recognition tasks. Hence, we can expect that the proposed approach may be useful for mulitimodal biometric system having palmprint, fingerprint and iris recognition capabilities.

VI. Acknowledgment

Portions of the research in this paper use the PolyU palmprint database collected by Hong Kong Polytechnic University.

References

[1] D. Zhang, *Palmprint Authentication*. Kluwer Academic Publication, 2004.

[2] D. Zhang, W.-K. Kong, J. You, and M. Wong, "Online palmprint identification," *IEEE Trans. Pattern Anal. Machine Intell.*, vol. 25, no. 9, pp. 1041–1050, Sept. 2003.

[3] C. D. Kuglin and D. C. Hines, "The phase correlation image alignment method," *Proc. Int. Conf. Cybernetics and Society*, pp. 163–165, 1975.

[4] K. Takita, T. Aoki, Y. Sasaki, T. Higuchi, and K. Kobayashi, "High-accuracy subpixel image registration based on phase-only correlation," *IEICE Trans. Fundamentals*, vol. E86-A, no. 8, pp. 1925–1934, Aug. 2003.

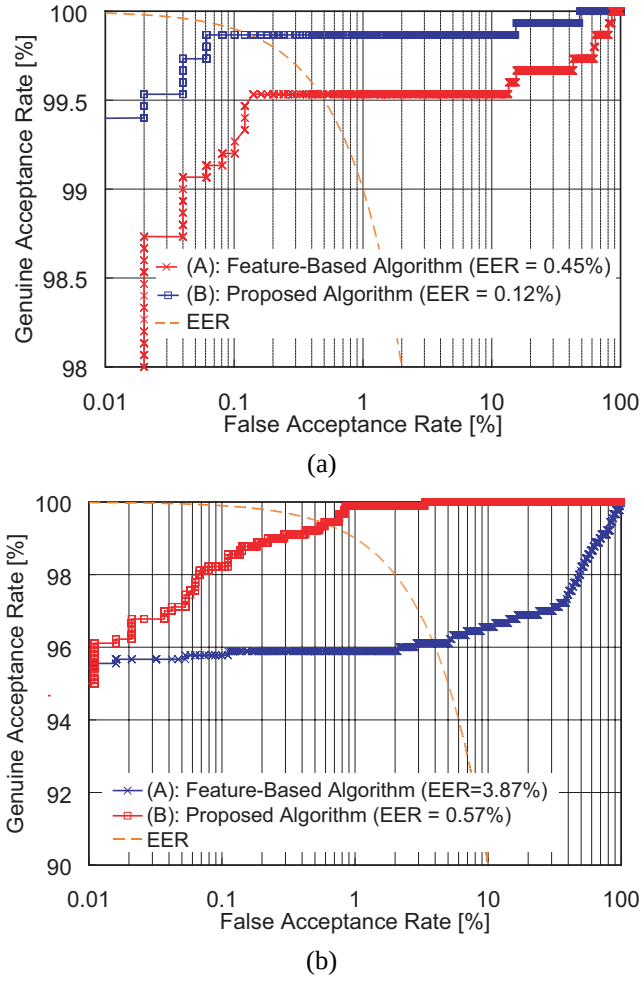

Fig. 4. ROC curves and EERs: (a) DB_A and (b) DB_B.

[5] K. Takita, M. A. Muquit, T. Aoki, and T. Higuchi, "A sub-pixel correspondence search technique for computer vision applications," *IEICE Trans. Fundamentals*, vol. E87-A, no. 8, pp. 1913–1923, Aug. 2004.

[6] K. Ito, H. Nakajima, K. Kobayashi, T. Aoki, and T. Higuchi, "A fingerprint matching algorithm using phase-only correlation," *IEICE Trans. Fundamentals*, vol. E87-A, no. 3, pp. 682–691, Mar. 2004.

[7] K. Ito, A. Morita, T. Aoki, T. Higuchi, H. Nakajima, and K. Kobayashi, "A fingerprint recognition algorithm combining phase-based image matching and feature-based matching," *Lecture Notes in Computer Science (ICB2006)*, vol. 3832, pp. 316–325, Dec. 2005.

[8] H. Nakajima, K. Kobayashi, M. Morikawa, A. Katsumata, K. Ito, T. Aoki, and T. Higuchi, "Fast and robust fingerprint identification algorithm and its application to residential access control products," *Lecture Notes in Computer Science (ICB2006)*, vol. 3832, pp. 326–333, Dec. 2005.

[9] Products using phase-based image matching. [Online]. Available: http://www.aoki.ecei.tohoku.ac.jp/research/poc.html

[10] K. Miyazawa, K. Ito, T. Aoki, K. Kobayashi, and H. Nakajima, "An efficient iris recognition algorithm using phase-based image matching," *Proc. the 2005 IEEE Int. Conf. Image Processing*, pp. II–49–II–52, Sept. 2005.

[11] K. Miyazawa, K. Ito, , T. Aoki, K. Kobayashi, and H. Nakajima, "A phase-based iris recognition algorithm," *Lecture Notes in Computer Science (ICB2006)*, vol. 3832, pp. 356–365, Dec. 2005.

[12] PolyU palmprint database. [Online]. Available: http://www4.comp.polyu.edu.hk/ biometrics/